A Scheme for Pixel-Scale Aerodynamic Surface Temperature over Hilly Land

MIN Wenbin*[1] (闵文彬), CHEN Zhongming[1] (陈忠明), SUN Linsheng[1] (孙林生), GAO Wenliang[1] (高文良), LUO Xiuling[1] (罗秀陵), YANG Tingrong[2] (杨廷荣), PU Jian[2] (蒲 剑), HUANG Guanglun[2] (黄光伦), and YANG Xiurong[3] (杨秀蓉)

[1] *The Institute of Plateau Meteorological Sciences, China Meteorological Administration, Chengdu* 610072

[2] *Meteorogical Bureau of Lezhi County, Sichuan, Lezhi* 641500

[3] *Sichuan Agrometeorological Center, Chengdu* 610072

(Received 6 December 2002; revised 4 November 2003)

ABSTRACT

Hilly-land satellite pixel-scale aerodynamic surface temperatures (AdST) are investigated using LAS (Large Aperture Scintillometer) and meteorological observations during 21–22 May 2001, indicating that the calculated temperatures are predominantly subject to estimated roughness lengths and, to a less extent, to estimated Bowen ratios, with errors to within 3.0 K between the AdST calculations and hilly radiometric surface temperatures retrieved from satellite data with the split window model. The errors depend heavily on the model used and the zenith angles and azimuth of the satellite and sun with respect to the observational site.

Key words: aerodynamic surface temperature, large aperture scintillometer, radiation temperature, sensible heat flux

1. Introduction

Aerodynamic surface temperatures (AdST) are an important parameter in numerical weather prediction, air-earth exchange, and monitoring large-scale evaporation, evapotranspiration, and dryness. At present, only a limited number of weather and ecological stations have single-point short-term AdST experimental data, but we are without such records on a weather satellite pixel-scale. For lack of such data, many branches for research and applications adopt other types of temperatures instead. In models dealing with telemetric-information monitoring extensive evapotranspiration, evaporation, and soil moisture, mixed pixel-scale AdSTs are replaced by radiometric surface temperatures (RmST), with replacement-resulting errors reduced by modifying aerodynamic resistance (Jupp et al., 1998). In synoptic analysis, AdSTs required for calculating sensible heat flux come from 0-cm level station temperature, with replacement produced error decreased by use of a drag coefficient. For homogeneous and isothermal surfaces, definitions of temperatures, aerodynamic, radiometric, and thermodynamic are all equivalent. But over the opposite-type surfaces there is no thermodynamic surface temperature available for measuring molecular mean kinetic energy, leading to the difference between AdST and RmST. Satellite data-retrieved RmSTs are those from sensor-received surface-emitted thermal infrared radiation through inverse calculation by the Planck function while AdSTs come from the inverse operation of the sensible heat flux term of the surface heat balance expression. Although the AdST differs from satellite data-reduced pixel-scale RmST, their energy originates in solar incident radiation and their interface is the earth's surface, leading to an intrinsic relation between them. Currently, satellite data-retrieved regional and global RmSTs have the scales they do because they meet the needs of parameters in weather forecasting, offering irreplaceable information in large quantities. Hence, to make the approach to use satellite-obtained RmST as a parameter is a leading subject of great usefulness to the improvement of numerical weather forecasting preci-

*E-mail: qxkysmwb@mail.sc.cninfo.net

sion. Models for gaining land pixel-scale RmST in current use include radiation transmission, split window, LSF conceptual, single-channel, multi-channel, multi-angle/multi-channel models, etc. The retrieval accuracy of land pixel-scale RmST is affected by the correction of the atmospheric effect, unknown surface emissive rate, space inhomogeneity, and skin effect of RmST (Li et al., 1999, 2001; Wang, 2001). All models of this kind have limitations, and now we have no universality for any area.

Definitions of pixel-scale "true temperature" are many, depending on the study region (Becker and Li, 1995). For the purposes of earth-air exchange and weather forecasting, the pixel-scale AdST is regarded as "true temperature" with which to assess the models for retrieving RmST and AdST applicable to a given region. For this reason, this article is devoted to the development of a calculation scheme applicable to hilly land of Sichuan for AdST matching polar orbiting satellite (POS) pixel-scale data, and in the context of the scheme, pixel-scale AdSTs are found by means of the near-surface layer logarithmic flux profile from Monin-Obukhov similarity theory and large aperture scintillometer(LAS)-measured larger-scale (horizontal length of 2 000 m, close to the satellite pixel scale) sensible heat flux, turbulent temperature scale, and frictional winds in the near surface layer as well as station meteorological data, followed by the comparison of estimated AdST to reduced pixel-scale RmST.

2. Principles and method

AdST refers to air temperature that is displaced by extrapolation onto a zero plane via the air temperature profile plus roughness height. Let us first examine the profile in the near-surface layer.

2.1 *The air temperature profile*

The paper is confined to the investigation of the case of unstable stratification in close association with weather changes. The techniques of measuring and calculating turbulence flux are many. Here only the aerodynamic technique is introduced.

Following Monin-Obukhov similarity theory, under the assumptions of homogeneity and steadiness of the surface, the dimensionless profile of a meteorological element in the near-surface layer is denoted by a universal function $\phi(Z/L)$ (Chen et al., 1983), viz.,

$$\frac{\partial \overline{u}}{\partial Z}\frac{kZ}{u_*} = \phi_m\left(\frac{Z}{L}\right) , \tag{1}$$

$$\frac{\partial \overline{\theta}}{\partial Z}\frac{kZ}{\theta_*} = \phi_h\left(\frac{Z}{L}\right) , \tag{2}$$

$$u_* = \sqrt{\tau/\rho} , \tag{3}$$

$$\theta_* = -\frac{H}{\rho c_p u_*} , \tag{4}$$

$$L = \frac{T}{kg}\frac{u_*^2}{\theta_*} = -\frac{\rho c_p T}{kg}\frac{u_*^3}{H} , \tag{5}$$

in which ϕ_h and ϕ_m are universal function for sensible heat and momentum respectively, u_*, θ_*, and L are the frictional wind, temperature scale, and Obukhov length, respectively; u, θ, Z, and k (=0.4) represent wind speed, potential temperature, height, and the Von Karman constant, in order; τ, ρ, c_p, H, T, and g signify, respectively, momentum, air density, specific heat at constant pressure, sensible heat flux, mean layer temperature, and gravitational acceleration.

Since the flux profile depends upon dimensional analysis, the universal function $\phi(Z/L)$ relies on experimental data. The mathematical expression for the function over a smooth and homogeneous surface in most of today's references is given as follows (Chen et al., 1983):

In an unsteady stratification ($L<0$ or $H>0$, usually during daytime hours)

$$\phi_h = \phi_m^2 = \left(1 - 16\frac{Z}{L}\right)^{-\frac{1}{2}} . \tag{6}$$

Assuming that t, H, u, L, k, and p do not change with height in the near-surface layer, we integrate (1) and (2), then obtain

$$\tau = \frac{\rho k u_*}{\int_{Z_1}^{Z_2}\frac{\phi_m}{Z}dZ}(u_2 - u_1) , \tag{7}$$

$$H = \frac{\rho c_p k u_*}{\int_{Z_1}^{Z_2}\frac{\phi_h}{Z}dZ}(\theta_1 - \theta_2) . \tag{8}$$

By integrating their denominators we have

$$\int_{Z_1}^{Z_2}\frac{\phi_h}{Z}dZ = \left[\ln\left(\frac{Z_2}{Z_1}\right) - \psi_H\left(\frac{Z_2}{L}\right) + \psi_h\left(\frac{Z_1}{L}\right)\right] , \tag{9}$$

$$\int_{Z_1}^{Z_2}\frac{\phi_m}{Z}dZ = \left[\ln\left(\frac{Z_2}{Z_1}\right) - \psi_m\left(\frac{Z_2}{L}\right) + \psi_m\left(\frac{Z_1}{L}\right)\right] , \tag{10}$$

$$\psi_m = 2\ln\left(\frac{1+x}{2}\right) + \ln\left(\frac{1+x^2}{2}\right) - 2\arctan x + \frac{\pi}{2} , \tag{11}$$

$$\psi_h = 2\ln\left(\frac{1+x^2}{2}\right) , \tag{12}$$

$$x = \left(1 - 16\frac{Z}{L}\right)^{\frac{1}{4}} , \tag{13}$$

and then we find the respective expressions of wind and temperature profiles and frictional velocity in the form

$$u_2-u_1=\frac{u_*}{k}\left[\ln\left(\frac{Z_2}{Z_1}\right)-\psi_m\left(\frac{Z_2}{L}\right)+\psi_m\left(\frac{Z_1}{L}\right)\right] , \quad (14)$$

$$\theta_2-\theta_1=\frac{\theta_*}{k}\left[\ln\left(\frac{Z_2}{Z_1}\right)-\psi_h\left(\frac{Z_2}{L}\right)+\psi_h\left(\frac{Z_1}{L}\right)\right] , \quad (15)$$

$$u_* = \frac{k(u_2-u_1)}{\ln\left(\frac{Z_2}{Z_1}\right)-\psi_m\left(\frac{Z_2}{L}\right)+\psi_m\left(\frac{Z_1}{L}\right)} . \quad (16)$$

Since the gradients of actual temperature are approximately equal to those of potential temperature in the near-surface layer (Weng et al., 1981), (15) can be rewritten as

$$T_2-T_1=\frac{\theta_*}{k}\left[\ln\left(\frac{Z_2}{Z_1}\right)-\psi_h\left(\frac{Z_2}{L}\right)+\psi_h\left(\frac{Z_1}{L}\right)\right] , \quad (17)$$

From (4), (16), and (17), we obtain

$$H=\frac{\rho c_p k^2(u_2-u_1)(T_1-T_2)}{\left[\ln\left(\frac{Z_2}{Z_1}\right)-\psi_m\left(\frac{Z_2}{L}\right)+\psi_m\left(\frac{Z_1}{L}\right)\right]\cdot\left[\ln\left(\frac{Z_2}{Z_1}\right)-\psi_h\left(\frac{Z_2}{L}\right)+\psi_h\left(\frac{Z_1}{L}\right)\right]} , \quad (18)$$

setting

$$r_{\rm a}=\frac{\left[\ln\left(\frac{Z_2}{Z_1}\right)-\psi_m\left(\frac{Z_2}{L}\right)+\psi_m\left(\frac{Z_1}{L}\right)\right]\cdot\left[\ln\left(\frac{Z_2}{Z_1}\right)-\psi_h\left(\frac{Z_2}{L}\right)+\psi_h\left(\frac{Z_1}{L}\right)\right]}{k^2(u_2-u_1)} . \quad (19)$$

As we know, an actual surface is not a smooth plane so that we have to take account of the height of the zero plane displacement d and roughness length Z_0. Thus, the variable x in (11), (12), and (13) for finding ψ_m and ψ_h is given as

$$x=\left(1-16\frac{Z-d}{L}\right)^{\frac{1}{4}} . \quad (20)$$

Following the definition, we know that AdST comes from the air temperature gained by extrapolating measurements onto a zero plane with the aid of the air temperature profile plus the roughness height (Z_0+d), and as the wind is zero at the height, Z_1 and Z_2 in the above expressions are replaced with (Z_0+d) and (Z_2-d), respectively. Now we return to (18), which can be simplified as

$$H=\frac{\rho c_p(T_1-T_2)}{r_{\rm a}} , \quad (21)$$

with T_1 representing the AdST.

2.2 *Principles of LAS-Obtained Sensible Heat Flux and AdST*

The LAS is for measuring sensible heat flux in the unsteadily stratified near-surface layer and consists of a transmitter (emitting near-infrared radiation at wavelength $\lambda = 940$ nm) and a receiver spaced at a certain distance (typical optical path of 1000–3000 m).

The LAS has a limited optical diameter and light emitting diode (LED) size. The transmitting electromagnetic beams are composed of superimposed noncoherent spherical waves, which undergo refraction when passing through the atmosphere, with atmospheric refractivity fluctuating with the change in temperature, humidity, and pressure along the optical path. The refractivity has its structural functional parameter C_n^2 related to the temperature (humidity) structural parameter $C_T^2(C_q^2)$ in the following way (Hill et al., 1980):

$$C_n^2=A_T^2\frac{C_T^2}{T^2}+A_q^2\frac{C_q^2}{q^2}+2A_TA_q\frac{C_{Tq}}{Tq} . \quad (22)$$

The relationship between C and the LAS signal $(\sigma^2_{\ln I})$ takes the form (Wang et al., 1978)

$$C_n^2=1.12\sigma^2_{\ln I}D^{7/3}L^{-3} , \quad (23)$$

where D denotes the diameter of beams of LAS emitted rays and L the optical path. The second term on the right-hand side of (22) can be dropped and the third takes the form of the function of the Bowen ratio (β), assuming temperature relates to fluctuating humidity (De Bruin et al., 1995, 1996). Consequently, we have

$$C_T^2=C_n^2\frac{T^2}{A_T^2}\left(1+\frac{0.03}{\beta}\right)^{-2} , \quad (24)$$

$$A_T=-0.78\times10^{-6}\frac{p}{T} , \quad (25)$$

in which p is the pressure. Under unsteady stratification. C_T^2 is related to the temperature scale θ_* as follows:

$$\frac{C_T^2(Z_s-d)^{2/3}}{\theta_*^2}=C_{T1}\left(1-C_{T2}\frac{Z_s-d}{L}\right)^{-2/3} , \quad (26)$$

where Z_s represents the height of LAS beams above the ground, C_{T1} and C_{T2} the empirical constants, and the other symbols having the same meanings as mentioned. From (4), (5), and (16) we know θ_* (turbulent temperature scale), u_* (frictional wind), and

L (Obukhov length) are closely linked to H (sensible heat flux). H is acquired by means of estimated C_T^2, wind, temperature, zero plane displacement, and roughness length through iterative operations with (4), (5), (16), and (26), therefrom L is gained as well. Then, the relevant parameters are put into (21) to find AdST T_1. It follows from the above that LAS-based H is a regional mean at a certain scale so that the resulting AdST represents the areal mean at a scale that goes well with the pixel-scale of meteorological POS data, and thus comes the name of pixel-scale AdST.

2.3 *Retrieval of RmST from satellite data*

Concerning satellite data retrieval of RmST, Li et al. (1999, 2001) elucidated the fundamentals (principles, methods, models, and limitations), especially the scale effect of the Plank function and the scale correction using optical geometric models. Becker and Li (1995) explained the differently-defined surface temperatures. RmST is the temperature derived by the inverse of the Plank function

$$T_{sr} = B^{-1}\left(\frac{R_\lambda - (1-\varepsilon_\lambda)R_{at\lambda\downarrow}}{\varepsilon_\lambda}\right), \qquad (27)$$

where R_λ is radiance measured by a radiometer and $R_{at\lambda}$ is downward hemispheric atmospheric radiance, and ε_λ is surface emissivity. RmST is also called skin-felt temperature. For heterogeneous and non-isothermal surfaces, RmST and AdST are different and the skin temperature measured by a radiometer is no longer equal to the bulk temperature derived by a thermometer.

This paper deals with RmST retrieval in the context of the split window model proposed by Price (1984) and Becker and Li (1995) (Tian et al., 2000; Sobrino et al., 1994, 2001). Geographic correction is performed on AVHRR data with the model in such a way that, on an image of the AVHRR near-infrared channel (0.725–1.10 μm), the inflection points of the Minjiang River, Changjiang River, Tuojiang River, and Fujiang River are matched with their latitude-longitude digital representations as the initial correction, followed by precise correction with the Memorial Hall for Marshal Chen Yi (1200 m^2, to the west of the experimental site), the main streets of the City of Lezhi, and the weather station as the reference buildings. Those streets are in a cross-like arrangement, with the E-W street to the south of the experimental site that covers 6 pixel scales, the other spanning one only. On a thermal infrared image (10.3–11.3 μm), the crossed streets are bands of high-value temperatures, with radiometric measurements 5–6 K higher than in the neighboring rural areas. Over 1 km^2 around the weather station is a rural area where pixel-scale temperatures (including the station itself) are 5–6 K lower than those derived at the Hall and main streets. The three ground objects are visible on satellite imagery, with the site-related pixel located to the due north of the station pixel. The study employs these object-associated satellite images for precise geographic correction of site-related images, with errors smaller than those of sub-pixel scale of < 500 m (Xu et al., 1994).

Cloud monitoring of the LAS observing site-related pixel scale was made using the APOLLO scheme (AVHRR Processing scheme over cloudy land and ocean) developed chiefly by Saunders and Kriebel (1988) and Kriebel et al. (1989).

The NDVI (Normalized difference vegetation index) model of Sobrino et al. (2001) is employed to compute pixel emissivity of Channels 4 and 5. Prior to NDVI calculation, we make atmospheric correction of the reflectivity of Channels 1 and 2 by dint of the Simplified Method for the Atmospheric Correction (SMAC) program (Rahmam and Dedien, 1994). The SMAC-required pixel-scale vapor content in an air column throughout the troposphere comes from the dew-point measurements derived at the weather station of Lezhi County by means of the dew-point retrieval scheme developed by Yang and Qiu (2001). As for the aerosol optical thickness (wavelength of 550 m), it is found by

$$\text{Optical thickness} = \ln(50)/\text{visibility} - 0.01159\ . \qquad (28)$$

The reguired elevated angle and azimuth of the satellite and sun with respect to the observing site are derived through auto-programming and calculation, with the formulae and parameters given in Chen and Jia (1992), Xia et al. (1955), Wang (2001), and Xu et al. (1994) and with the real-time data from the National Satellite Meteorological Center of the China Meteorological Administration. The AVHRR data and POS orbit parameters are provided by the related microcomputer system developed by the Center as well.

3. Brief description of the observations

The experimental site was inside Lezhi County of central Sichuan Province, marked by typical hilly landform, and thus well applicable to the monitoring and research of air-earth interactions over hilly land. In addition to conventional meteorological instruments, we made use of a LAS as a remotely sensing device for pixel-scale sensible heat flux. The meteorological instruments were mounted at the observational field (30.17°N, 105.02°E) and the LAS receiver at an iron tower, ~20 m above ground at 480 m MSL, within the County Meteorological Bureau, with its transmitter on a mound (532 m MSL) 2190 m away due north of the

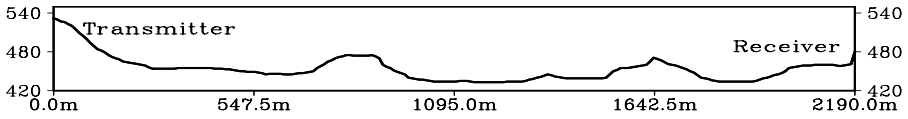

Fig. 1. The path between the LAS transmitter and receiver.

Bureau, as shown in Fig. 1. The underlying surface over the LAS path is characterized by (starting from the transmitter) trees (0–130 m), dry land (130–270 m), watered fields (270–330 m), dry land (330–530 m), watered fields (530–650 m), dry land (650–770 m), mulberry forest (770–900 m), dry land (900–960 m), vegetable plots (960–1080 m), watered fields (1080–1290 m), vegetable fields (1290–1400 m), dry land (1400–1500 m), trees (1500–1780 m), watered plots (1780–1930 m), vegetable plots (1930–2030 m), and trees (2030–2190 m). The observation was carried out from 16 April 2000 to 31 October 2001. The conventional measurements include auto-recorded pressure, temperature, humidity, and rainfall together with man-made observations at 0800, 1400, and 2000 Beijing Time (BT). Also made were measurements of soil-surface temperature, cropland soil moisture, and normalized agrometeorological elements. The LAS is an auto-recorder, giving data at a 10-min interval which form the mean information over the 2000 m distance.

4. Results and analysis

For synoptic forecasting purposes, a spell of fine days is necessary for gaining good-quality LAS and POS data. Thus, we decided on 21–22 May 2001. With cloud cover present in the following two days we had POS data from satellites NOAA 11, 14, 16, and AVHRR. The reference height temperatures are of in-screen origin. The air temperatures and humidities matching those during the LAS operation are acquired by interpolating the related measurements from the thermo-hygrograph and regular station observations. The winds and pressures in relation to those during the LAS operation are derived by interpolating measurements made regularly at the station. The anemograph is 10.7 m above the surface and the LAS is 59.2 m above the ground.

We now deal with the determination of the zero-plane displacement height and roughness length. The spring of 2001 was severely dry in the region. On 21–22 May, wheat was harvested and sweet potatoes are not yet planted, with scattered corn seedlings, ∼0.18 m high on the land and no rice seedlings available in plots because of lock of water. Following Choudhury et al. (1986), we defined the zero-plane displacement to be zero and roughness length to be 0.0234 m after many tests.

Now we present the data and analysis below.

(1) Meteorological and LAS data during the POS passage (Table 1).

(2) Calculated sensible heat fluxes, AdST, and Obukhov length (Table 2).

Table 1. Meteorological and LAS data on 21–22 May 2001 during POS passage.

	hour							C_T^2			
day	start	end	T_2	u_2	p	C_n^2	Quality	$\beta = 1$	$\beta = 0.65$	$\beta = 0.3$	$\beta = 10 \times 10^7$
141	14.6667	14.833	306.86	2	950.3	1.71×10^{-14}	1	0.0260	0.0252	0.0228	0.0274
141	14.8333	15	306.86	2	950.3	1.99×10^{-14}	1	0.0303	0.0293	0.0265	0.0318
141	17.5	17.667	307.16	2.5	949.7	4.28×10^{-15}	1	0.0066	0.0063	0.0057	0.00679
142	14.5	14.667	307.46	3	949.7	1.88×10^{-14}	1	0.0289	0.0280	0.0253	0.0308
142	17.6667	17.833	308.46	2.5	948.7	2.03×10^{-15}	1	0.0032	0.0031	0.0028	0.00328

Table 2. Calculations of sensible heat fluxes, ADST and Obukhov length on 21–22 May 2001.

	hour		H				Aerodynamic Temperature Suraces				Obukhov length		
day	start	end	β=1	β=0.65	β=0.3	β=10×10^7	β=1	β=0.65	β=0.3	β=10×10^7	β=1	β=0.65	β=0.3
141	14.67	14.83	429.0	419.1	388.7	448.4	318.91	318.71	318.09	319.30	–1.64	–1.67	–1.76
141	14.83	15.00	480.6	469.5	435.5	502.4	319.93	319.71	319.04	320.34	–1.52	–1.55	–1.63
141	17.50	17.67	152.4	148.9	138.1	159.3	312.41	312.32	312.02	312.60	–5.45	–5.54	–5.85
142	14.50	14.67	462.6	451.9	419.2	483.5	319.18	318.97	318.33	319.58	–3.62	–3.68	–3.89
142	17.67	17.83	87.9	85.8	79.6	91.8	311.86	311.79	311.60	311.98	–8.20	–8.35	–8.84

(3) Comparison of the averaged AdST calculations to the station surface and air temperatures shows a great difference between them but closeness in terms of the averages of the latter two (refer to Table 3).

(4) AdST depends predominantly upon estimated roughness length and, to a less extent, upon the calculated Bowen ratio. For instance, between 1730–1740 BT 21 May, the AdST increases by about 4 K when the estimated roughness length decrease from 0.3 to 0.0234 m, which occurs because of a small skewness of the temperature profile in the layer immediately close to the ground. And when the calculated Bowen ratio is increased from 0.3 to 10 000 000, the ADST increases from 312.02 to 312.60 K, a rise of only 0.58 K (the calculations are given in Tables 3 and 4).

(5) Over the study terrain and underlying surface, the differences are mostly <3 K between mean AdST and satellite retrieved pixel-scale RmST at the same time, and the differences are related to the model used, and the zenith angle and azimuth of the satellite and sun (Li et al., 1999, 2000). The radiometric data listed in Tables 5 and 6 are reduced from the split window model proposed by Price (1984) and Becker and Li (1995). The split window model of Becker and Li (1995) is intended to determine the relevant parameters of satellite NOAA 14, and the RmSTs derived

Table 3. Mean AdST versus station surface and air temperature.

	hour			Aerodynamic temperature surfaces				
day	start	end	T_s	$\beta = 1$	$\beta = 0.65$	$\beta = 0.3$	$\beta = 10 \times 10^7$	T_2
141	14.6667	14.833	333.9	318.91	318.71	318.09	319.30	306.86
141	14.8333	15	333.9	319.93	319.71	319.04	320.34	306.86
141	17.5	17.667	319.1	312.41	312.32	312.02	312.60	307.16
142	14.5	14.667	333.8	319.18	318.97	318.33	319.58	307.46
142	17.6667	17.833	319.2	311.86	311.79	311.60	311.98	308.46

* For the meanings of the symbols see the text. T_2, u_2, and p are in units of K, m s^{-1}, and hPa, respectively. T_s and T_2 denote temperature measured at the ground and in shelter, respectively.

Table 4. Close relation between AdST and roughness length.

		Aerodynamic temperature surfaces				
duration	T_2	Z_0=1.0 m	Z_0=0.7 m	Z_0=0.3 m	Z_0=0.0234 m	β
17.50–17.6667	307.16	307.4	307.7	308.5	312.41	1.0

*Z_0 is the roughness length.

Table 5. Mean AdST in comparison to split window-retrieved RmST.

	hour		Aerodynamic temperature surfaces				Radiometric temperature surfaces	
day	start	end	$\beta = 1$	$\beta = 0.65$	$\beta = 0.3$	$\beta = \times 10^7$	Becker and Li (1995) method	Price (1984) method
141	14.8333	15	319.93	319.71	319.04	320.34	321.4	319.5
141	17.5	17.6667	312.41	312.32	312.02	312.60	310	310
142	14.5	14.667	319.18	318.97	318.33	319.58	323.8	322.5
142	17.6667	17.8333	311.86	311.79	311.60	311.98	312	312

Table 6. Satellite passage time, observing angle, and solar incident angle.

			satellite		sun	
day	satellite	passage	zenith angle (°)	azimuth angle (°)	zenith angle (°)	azimuth angle (°)
141	NOAA16	14:50′35″	32.9701	232.6019	27.5844	255.3281
141	NOAA12	17:36′23″	14.8528	136.9204	63.1214	278.8149
142	NOAA16	14:39′56″	24.2779	199.8464	25.2667	253.1044
142	NOAA14	17:49′8″	25.506	240.0487	65.7397	280.3979

from their model using NOAA/AVHRR data are close to the mean AdSTs (see Line 4 of Table 5, at 17.667 to 17.833 h BT of day 142). However, in the case of NOAA-16/AVHRR data, the difference is as much as 4.2 K (see Line 3 of Table 5 for 14.5 to 14.667 h BT of day 142).

5. Concluding remarks

In the context of LAS and meteorological measurements we are permitted to calculate averaged AdST on a POS pixel-scale over hilly land. The AdST depends dominantly on estimated roughness length and to a less degree on the calculated Bowen ratio. Experiments show that pixel-scale RmSTs retrieved by the split window model of Price (1984) and Becker and Li (1995) differ from mean AdSTs mostly by $\langle 3$ K, which are closely related to the model and the zenith angle and azimuth of the satellite and sun with respect to the observing site.

Over heterogeneous and non-isothermal surfaces, RmSTs differ greatly from AdSTs, but both have energy from solar radiation and the ground as their interface, thus suggesting their intrinsic relation. For a given region whose terrain and underlying surface features are almost unchanged, greater possibilities may be available as regards to the evolution of the differences between the two factors. Hence, further research remains to be done by means of large volumes of data.

Acknowledgments. The authors are grateful to Academician Li Xiaowen, Prof. Li Zhaoliang, Senior Researcher Zhang Renhua and Drs. Wang Pengxin and Liu Shaomin for their valuable assistance and comments. This work was supported jointly by the Special Funds for Major State Basic Research Project (Grant No. G2000077900) and Sino-Holland Cooperative Research CEWBMS.

REFERENCES

Becker, F., and Li Zhaoliang, 1995: Surface temperature and emissivity at various scales: Definition, measurement and related problems. *Remote Sensing Review*, **12**, 225–253.

Chen Wanlong, Weng Duming, and Sun Weiguo, 1983: A diagraph of turbulent coefficients for integral. *J. Nanjing Inst. Meteor.*, **1**, 127–129.

Chen Fangyun, and Jia Neihua, 1992: *A Handbook of Observing and Controlling Satellites*. China Science Press, Beijing, 556pp.

Choudhury, B. J., R. J. Reginato, and S. B. Idso, 1986: An analyses of infrared temperature observation over wheat and calculation of latent heat flux. *Agricultural and Forest Meteorology*, **37**, 75–88.

De Bruin, H. A. R., B. J. M. Van den Hurk, and W. Kohsiek, 1995: The scintillation method tested over a dry vineyard area. *Bound.-Layer Meteor.*, **76**, 25–40.

De Bruin, H. A. R., J. P. Nieveen, S. F. J. de Wekker, and B. G. Heusinkveld, 1996: Large aperture scintillometry over a 4.8 km path for measuring areally-average sensible heat flux. Proc. 22$^{\text{nd}}$ *AMS Symposium on Agricultural and Forest Meteorology*, 28 January–2 February, Atlanta Georgia, USA.

Hill, R. J., S. F. Clifford, and R. S. Lawrence, 1980: Refractive-index and absorption fluctuations in the infrared caused by temperature,humidity and pressure fluctuations. *J. Opt. Soc. Am.*, **70**, 1192–1205.

Jupp, David L. B., Tian Guoling, Tim R. McVicar, Qin Yi, and Li Fuqin, 1998: Soil moisture and drought monitoring using remote sensing 1: Theoretical background and methods, EOC Report.

Kriebel, K. T., R. W. Saunders, and G. Gesell, 1989: Optical properties of clouds derived from fully cloudy AVHRR pixels. *Contrib. Phys. Atmos.*, **62**, 165–171.

Li Xiaowen, Wang Jindi, and A. H. Strahler, 1999: Plank scale-effects of non-isothermal black body surface. *Sciences of China in* (*E*), **29**(5), 422–426.

Li Xiaowen, Wang Jindi, and A. H. Strahler, 2000: Scale effects and scaling-up by geometric-optical model. *Science in China* (*E*), **30** (Suppl.), 12–17.

Li Xiaowen, Wang Junfa, Wang Jindi, and Liu Qinhuo, 2001: *Multi-Angles Thermal Infrared Remote Sensings of Underlying Surface.* Science Press, Beijing, 214pp.

Price, J. C., 1984: Land surface temperature measurements from the spilt window channels of NOAA 7 advanced very high resolution radiometer. *J. Geophys. Res.*, **89**, 7231–7237.

Rahman, H., and G. Dedieu, 1994: SMAC: A simplified method for the atmospheric correction of satellite measurements in the solar spectrum. *Int. J. Remote Sens.*, **15**, 123–143.

Saunders，R. W., and K. T. Kriebel, 1988: An improved method for detecting clear sky and cloudy radiances from AVHRR data. *Remote. Sens.*, **9**, 123–150.

Sobrino, J. A., Li Zhaoliang, M. P. Stoll, and F. Becker, 1994: Improvements in the split-windows technique for land surface temperature determination. *IEEE Trans. Geosci. Remote Sens*, **2**, 243–253.

Sobrino, J. A., N. Raissouni, and Li Zhaoliang, 2001: A comparative study of land surface emissivity retrieval from NOAA Data. *Remote Sens. Environ.*, **75**, 256–266.

Tian Guoliang, Xu Xingkui, and Liu Qinhuo 2000: A model of dynamic surface characteristics for surface energy exchange. *J. Remote Sensings*, **4**(suppl.), 121–128.

Wang Pengxin, 2001: Research of the soil moisture sensing model for a region typical of the Loess Plateau of China. Ph. D. dissertation, Wuhan University.

Wang Tingyi, G. R. Ocha, and S. F. Clifford, 1978: A saturation-resistant optical scintillometer to measure C_n^2. *J. Opt. Soc. Am.*, **68**, 334–338

Weng Duming, Chen Wanlong et al., 1981: *Microclimate and Its Cropland Version.* China Agricultural Press, Beijing, 356pp.

Xia Jianbai et al. (Eds), 1955: *Practical AdSTronomy*, Commercial Press, Shanghui, Ltd, 260pp. (in Chinese)

Xu Jianmin et al. (translators), 1994: *Meteorological satellite System and data with their applications to environments.* China Meteorological Press, Beijing. (in Chinese)

Yang Jingmei, and Qiu Jinhuang, 2002: A merthod for estimating precipitable water and effective water vapor contert from ground humidity parameters. *Chinese J. Atmos. Sci.*, **26**(1), 81–96.